Journal of Physics: Conference Series **2877** (2024) 012113 doi:10.1088/1742-6596/2877/1/012113

Shadows and signals: a brief history of medical imaging

Martin J. Graves

Department of Radiology, University of Cambridge, Addenbrooke's Hospital, Cambridge Biomedical Campus, Hills Road, Cambridge CB2 0QQ, UK

E-mail: mjg40@cam.ac.uk

Abstract. Medical imaging is a revolutionary field that has transformed healthcare, providing clinicians with the ability to view the inside of the body without invasive procedures. This overview traces the evolution of the major medical imaging modalities from their inception to the advanced technologies used today. Starting with the serendipitous discovery of X-rays by Wilhelm Conrad Röntgen in 1895 the subsequent developments in various imaging modalities including fluoroscopy, computed tomography (CT), magnetic resonance imaging (MRI), nuclear medicine and ultrasound imaging are chronicled. The technological breakthroughs, pioneering scientists and clinicians involved, and the significant impact of these advancements on diagnostic medicine are discussed. Additionally the integration of digital imaging, artificial intelligence (AI) and machine learning technologies into medical imaging is considered together with their potential to revolutionise diagnostic procedures, enhance patient care and streamline healthcare delivery.

1. X-rays: The dawn of medical imaging

The history of medical imaging can be traced back to 1895 when Wilhelm Conrad Röntgen, a German Professor of Physics at the University of Würzburg accidentally discovered X-rays. Whilst performing experiments with a cathode ray tube covered by a shield of black cardboard he found that a piece of barium platinocyanide paper several feet away fluoresced. Further experimentation showed that there was a form of invisible light coming from the cathode ray tube. Since Röntgen could not explain this new type of rays he termed them 'X-rays', although colleagues subsequently named them Röntgen rays, a name that is still used in many languages. On Friday 8th November 1895 he performed the first in vivo X-ray of his wife's hand, showing that these X-rays could pass through soft tissues but were stopped by bones and metal, creating a shadow on a photographic plate (figure 1) [1].

The attenuation of X-ray beams as they pass through a material occurs due to the absorption of X-ray photons by the atoms in the material. The degree of attenuation depends on the material's thickness, density, atomic number and the X-ray's energy. Different tissues in the body attenuate X-rays differently, allowing for the creation of contrast in the X-ray images. X-rays were originally captured and viewed directly on photographic film, offering high spatial resolution but requiring chemical processing to develop and fix the film. The images were then viewed on lightboxes. With the development of digital imaging, and picture archiving and communications systems (PACS) there was a drive to eliminate film from the process. Computed radiography (CR) was invented by the Japanese company Fuji in the early 1980s. CR uses a cassette-based system with photostimulable phosphor plates that store the latent image, which is then scanned and digitised. Subsequently digital radiography (DR) was developed which captures images directly onto a digital detector, providing immediate access to the image, leading to a

faster and more efficient workflow compared to CR. A typical DR equipped X-ray room is shown in figure 2.

Figure 1. First medical X-ray by Wilhelm Röntgen of his wife Anna Bertha Ludwig's hand with a ring. By Wilhelm Röntgen - Source 1: [1]. Source 2: [2], Public Domain, https://commons.wikimedia.org/w/index.php?curid=12354709 .

The discovery of Röntgen/X- rays earned Röntgen the first Nobel Prize in Physics in 1901 with the citation "*in recognition of the extraordinary services he has rendered by the discovery of the remarkable rays subsequently named after him*". Within a month surgeons in Europe and the US were using radiographs to guide their operations and within six months radiographs were being used in the battlefield to locate bullets in wounded soldiers. Although Röntgen refused to take out patents on his discovery, many others claimed patents on improving the process and practicalities of creating X-rays. Early commercial entities included Siemens & Halske, a German engineering company that subsequently became part of Siemens.

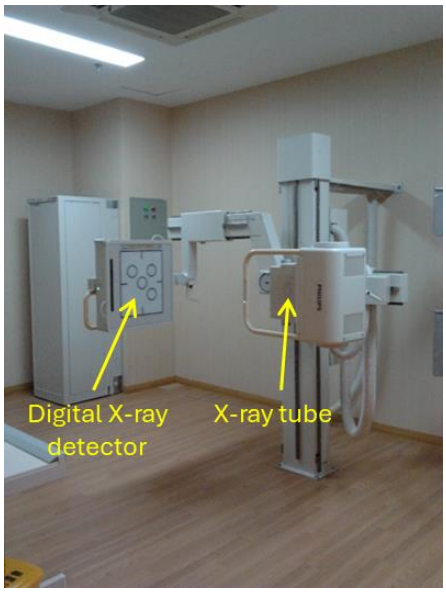

Figure 2. A modern DR X-ray room showing the X-ray tube and a digital detector for a standing patient. Ptrump16 (https://commons.wikimedia.org/wiki/File:Dedicated_chest_x-ray_room.jpg), Added annotation by Martin Graves, https://creativecommons.org/licenses/by-sa/4.0/legalcode.

2. Fluoroscopy: Watching the body in motion

On 5th February 1896 both Italian scientist Enrico Salvioni (with his "cryptoscope")[2] and William Francis Magie of Princeton University (with his "Skiascope")[3] independently developed live X-ray imaging apparatuses employing barium platinocyanide screens. Concurrently American inventor Thomas Edison determined calcium tungstate to be the most efficient fluorescent material. By May 1896 he had produced the first commercially viable device, known as the "Vitascope," later renamed the fluoroscope[4]. X-ray fluoroscopy allowed real-time imaging of the body's internal structures, making it possible to view movements and processes such as the digestive system in action. However, early fluoroscopy exposed patients and operators to high doses of X-ray radiation, necessitating the development of safer practices and equipment.

Modern real-time X-ray imaging is called radiographic fluoroscopy (RF). Many RF techniques involve the administration of an iodine-based contrast media into the body that absorbs X-rays. For example, the imaging of blood vessels known as angiography requires a small catheter to be inserted into an arterial blood vessel and manipulated to the anatomy of interest, e.g. the origin of the aorta to visualise the coronary arteries. The X-ray contrast media is then injected through this catheter and the physician can monitor the movement of the contrast media through the vessels and identify any blockages, stenosis or abnormalities in real-time (figure 3). RF can also be used to guide catheters or other instruments through the vessels for diagnostic or therapeutic purposes. A barium swallow is a dedicated test of the pharynx, oesophagus and proximal stomach. In this case the patient drinks a thick white, chalky liquid containing barium sulphate that also absorbs X-rays. Using RF the clinician can view the movement of the barium through the pharynx and oesophagus as the patient swallows.

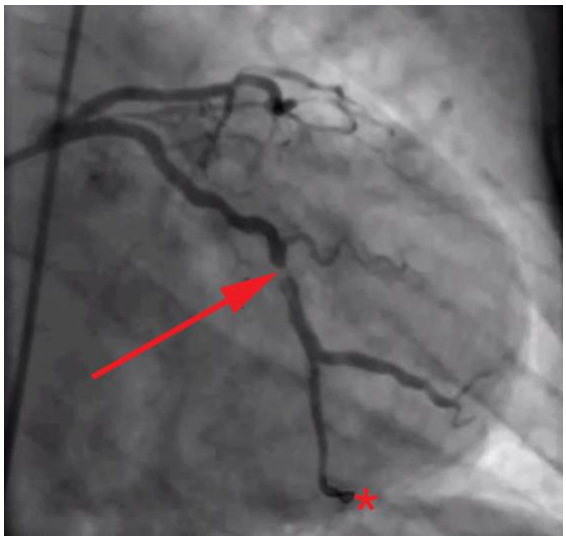

Figure 3. A single frame from a real-time X-ray coronary angiography procedure showing a partial occlusion (arrowed) of the left circumflex coronary artery. Todt T, Maret E, Alfredsson J, Janzon M, Engvall J, Swahn E (https://commons.wikimedia.org/wiki/File:Coronary_angiography_of_a_STEMI_patient,_showing_partial_occlusion_of_left_circumflex_coronary_artery.jpg), „Coronary angiography of a STEMI patient, showing partial occlusion of left circumflex coronary artery“, https://creativecommons.org/licenses/by/2.0/legal code .

3. Computed tomography (CT): A new dimension

The major limitation of conventional X-ray imaging is that the images are two-dimensional (2D) projections (shadows) of the tissues through which the beam passes. In 1959 William Oldendorf, an American neurologist conceived the idea of "*scanning a head through a transmitted beam of X-rays and being able to reconstruct the radiodensity patterns of a plane through the head*". Oldendorf had the idea by watching an engineer who was working on an automated apparatus to reject frostbitten fruit by detecting dehydrated portions. By 1961 he had completed a working prototype, using materials found in his home such as his son's toy train, a phonograph turntable and a spring motor from an alarm clock. He used a narrow beam of γ-ray radiation from a ^{131}I source that was detected by a sodium iodide (NaI)

crystal-photomultiplier with the scintillations counted by a ratemeter [5]. His test object comprised a block of plastic into which two concentric but irregularly spaced, rings of nails were inserted. The inner ring mimicked the brain and the outer ring the human skull. Oldendorf demonstrated that when the test object was rotated at 16 rpm and the centre of rotation moved at approximately 80 mm/hr, the acquired projection data showed that the nails positioned in the centre of the object were clearly discernible from the outer ring of nails. Oldendorf was successfully granted a patent for his idea on the 8th October 1963 [6]. Oldendorf spent three frustrating years trying to gain industrial interest in his original CT work [7]. He quit trying in 1964 when an X-ray equipment manufacturer told him that "*we cannot imagine a significant market for such an expensive apparatus which would do nothing but make a radiographic cross-section of a head*" [8].

Oldendorf's 1961 paper contained no mathematical detail of his method, but around the same time Allan MacLeod Cormack, a South African/American nuclear physicist was working on a side project to develop the mathematical underpinnings of a method to determine how a detailed picture of the internal structure of the human body could be obtained from projections created by X-ray or γ-ray radiation passing through the body. He published his work in two landmark papers in 1963 [9] and 1964 [10].

During the period 1967-19368 Godfrey Hounsfield, an electrical engineer working in the Central Research Laboratories (CRL) of the UK company EMI Ltd, also conceived of an idea to determine the contents of a three-dimensional (3D) box from a set of random readings taken through the box. Hounsfield simplified the reconstruction problem by considering the 3D object in the box as a stack of 2D slices rather than a 3D volume. Based upon his theoretical work Hounsfield generated an initial project proposal in 1968, however, there was no evidence that his concept for a 3D X-ray scanner would be useful clinically or even viable commercially. Furthermore EMI CRL was not prepared to provide any funding unless Hounsfield and his team could convince the Department of Health and Social Security (DHSS) to also provide some funding. On the basis that the DHSS required a preliminary technical report to consider funding Hounsfield wrote a new proposal in August 1968 requesting internal funding of £20,000 to perform the necessary work. The proposal was rejected but at the end of October 1968 Hounsfield was given £5,000 by EMI based on a verbal agreement from the DHSS that they would also contribute to the work. With the limited funding available Hounsfield like Oldendorf used a ^{95}Am γ-ray source and a NaI crystal-photomultiplier detector but set up his test rig using an old lathe bed. The various test objects were translated across the γ-ray beam and then rotated by 1°. This translate-rotate process was then repeated until the test object had been rotated 180°. The measured data was punched onto paper tape and fed into a large mainframe computer to perform a simple iterative reconstruction. The first test objects were initially simple Perspex and aluminium objects, followed by specimens of cows' brains and pigs' bodies obtained from an abattoir and ultimately a preserved section of a human brain. In July 1969 with a promise of further funding from the DHSS EMI increased the budget to £17,393 with the DHSS providing £5,000 in December 1996. These initial results were very encouraging and in January 1970 a decision was made to build a prototype head-only machine to acquire clinical images. The DHSS provided a further £7,419 in March 1970. There was, however, insufficient funding to build a prototype and EMI refused not only to fund any further work, but also demanded that their money to date be repaid. The issue was resolved when Hounsfield and his manager William ("Bill") Ingham persuaded Gordon Higson of the DHSS to place an order for four yet unbuilt scanners. The prototype was to be installed at Atkinson Morley's Hospital in Wimbledon (figure 4) and the three clinical systems were to be placed at the Hospital for Neurology and Neurosurgery in London, Manchester and Glasgow. The plan was that income from these machines would then fund a further system for Hounsfield and his team to continue their development work. The DHSS would also fund half of the remaining research costs in exchange for a small royalty on sales [11]. The DHSS probably made over £1 million in royalties.

The first clinical images were obtained using the prototype system on the 1st October 1971, although the images were not seen until the following day as the data had to be taken away and reconstructed on a mainframe computer back at the EMI CRL. Fortunately the minicomputer was being developed around the same time and a Data General Nova 820 minicomputer with 32K of memory, a 2.5-MB two-sided

hard drive, a reel-to-reel magnetic tape storage device and a printer was added to the system. Improvements to the image reconstruction were also developed including replacing Hounsfield's iterative algebraic reconstruction method with a much faster filtered back-projection algorithm.

At the 1972 annual meeting of the Radiological Society of North America (RSNA) Hounsfield and James Ambrose, the neuroradiologist at Atkinson Morley's Hospital gave a presentation on "*Computerized Axial Tomography*" immediately following the RSNA President's address. The scanner was also displayed in the commercial exhibition. The event was such a success that EMI took multiple orders for the scanner, each with a $100,000 non-refundable deposit [12].

Hounsfield and EMI had filed a patent on 23rd August 1968 [13] based upon the lathe-bed work. The US patent citing Oldendorf's 1963 patent [6] was filed on 27th December 1971 [14], but not granted until 11th December 1973 during which time the claims had been modified in light of Cormack's 1963 work. Hounsfield and Ambrose first described the system at the Annual Congress of the British Institute of Radiology in April 1972 [15] with two full articles published in 1973 with Hounsfield providing a technical description of the scanner (Hounsfield 1973) and Ambrose the clinical applications (Ambrose 1973).

Figure 4. EMI CT brain scanner installed at Atkinson Morley's Hospital, Wimbledon, London, UK in 1971 (the first used clinically) by EMI, Hayes, Middlesex, 1970-1971. Case courtesy of Raphael Ambros, Radiopaedia.org. From the case rID: 85113 .

Hounsfield continued to develop the scanner through several subsequent generations including the development of whole-body imaging and continual improvements in spatial resolution, acquisition time and true 3D volumetric acquisitions. By mid-1975 EMI had installed one hundred and sixty machines with an average cost of $400,000 [16].

Hounsfield received numerous awards, honorary degrees and decorations for his work. In 1967 he was awarded a CBE and in 1975 became a Fellow of the Royal Society. In 1979 he and Allan Cormack shared the 1979 Nobel Prize for Physiology or Medicine "*for the development of computer assisted tomography*". In 1981 Hounsfield was knighted by the Queen. He retired from EMI in 1986 and passed away on 12th August 2004 [17].

Throughout the 1980s and 1990s computerised tomography (CT) technology became more sophisticated. Scanners with even higher resolutions and faster scanning times were developed. The introduction of 'slip ring' technology allowed continuous rotation of the X-ray source and detectors (figure 5), which led to the development of spiral or helical CT in the late 1980s. This was a major development, allowing for entire organs to be imaged in a single breath-hold, vastly improving the comfort for patients and the quality of the images. The turn of the century saw the introduction of multislice CT scanners, capable of capturing multiple slices simultaneously, further reducing scan times and improving spatial resolution (figure 6).

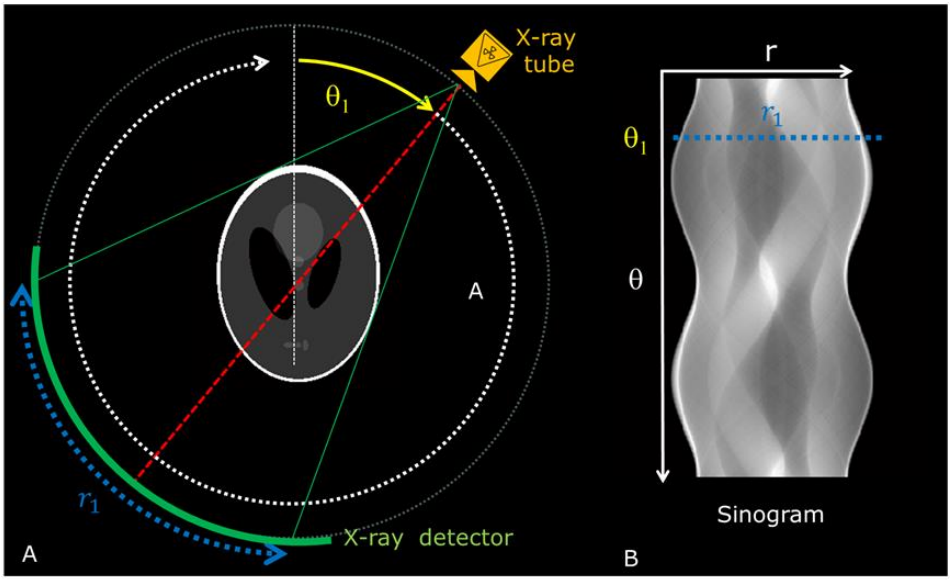

Figure 5. Basic principles of X-ray computerised tomography. In (A) the X-ray tube and detector rotate about the patient. At each rotation angle, e.g., θ_1, the X-ray projection (r_1) is sampled and is shown as a line intensity in the sinogram (dotted blue line). As the CT rotates the sinogram (B) is built up from the r profiles at each angle θ.

Today CT technology continues to evolve [18]-[20]. Advances in detector technology, image reconstruction algorithms and machine learning are making scans faster and safer (by reducing radiation dose) and providing functional as well as morphological information. Three-dimensional reconstructions and CT angiography are now commonplace, and the integration of PET (Positron Emission Tomography) with CT has led to PET/CT scanners that can show both anatomic and metabolic activity within the body.

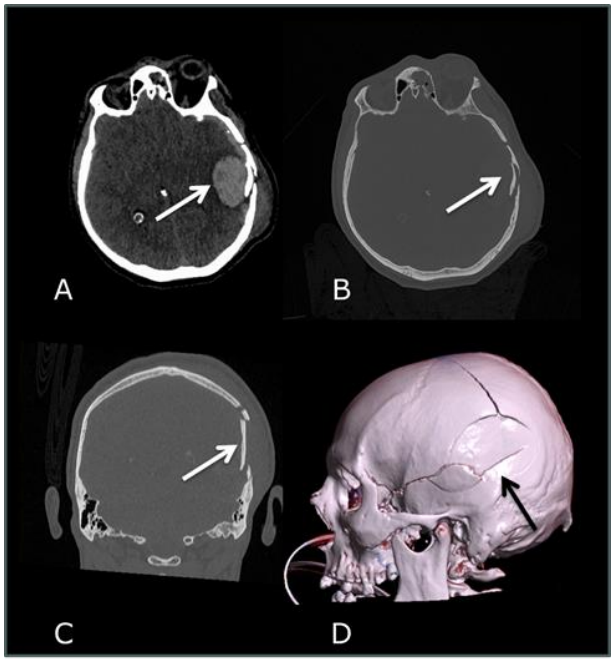

Figure 6. CT scan of a patient who has suffered a traumatic injury to their head. A) shows an axial slice through the brain demonstrating a severe intracranial bleed (arrow). B) shows the same slice but with the window level and width changed to demonstrate the skull. A depressed fracture of the bone can be seen (arrow). C) is a reformat in the coronal plane of the axial slices through the head. The fracture is seen more clearly (arrow). D) is a 3D rendering of the CT data producing a shaded surface display of the skull where the 3D anatomy of the skull fracture is demonstrated (arrow).

The most recent technological development is photon-counting CT where a new generation of highly sensitive detectors based on cadmium telluride (CdTe), cadmium zinc telluride (CZT) or silicon (Si) can count each individual photon that passes through the body and measure its energy [21]. This allows further reduction in radiation dose, enhanced image contrast and the capability to perform material-specific imaging. This latter ability enhances the diagnosis and characterisation of various pathologies by allowing clinicians to differentiate between, for example, the constituents of atherosclerotic plaque or the composition of kidney stones.

4. Magnetic resonance imaging (MRI): A magnetic leap forward

Magnetic resonance imaging (MRI) was developed in the late 1970s and early 1980s, and provided superior soft tissue contrast compared to CT. The principles of MRI are completely different from any other imaging modality. MRI is based upon the phenomenon of nuclear magnetic resonance (NMR) that was discovered by Felix Bloch working at Stanford [22] and Edward Purcell working at Harvard [23] almost simultaneously in 1946. They were subsequently awarded the 1952 Nobel Prize in Physics for "*the development of new methods for nuclear magnetic precision measurements and discoveries in connection therewith*". *The Boston Herald* reported that Purcell's discovery '*wouldn't revolutionize industry or help the housewife*'. Bloch, a Swiss-born Jew and friend of quantum physicist Werner Heisenberg, quit his post in Leipzig in 1933 in disgust at the Nazis' expulsion of German Jews (as a Swiss citizen, Bloch himself was exempt). Bloch's subsequent career at Stanford was crammed with major contributions to physics and he has been called the father of solid-state physics. The initial concept for the medical application of NMR originated with Raymond Damadian in 1971. He and his colleagues at the State University of New York Health Science Center, who were starved of mainstream research funding, even went so far as to design and build their own superconducting magnets operating in their Brooklyn laboratories. The first human NMR image is attributed to them. NMR imaging of two tubes of water using a magnetic field gradient was first demonstrated by Paul Lauterbur at the State University of New York at Stony Brook in 1973. His seminal paper "*Image formation by induced local interactions, examples employing nuclear magnetic resonance*" [24] was originally rejected. However, thirty years later *Nature* placed this work in a book of the twenty one most influential scientific papers of the 20th century.

MRI primarily looks at the nucleus of hydrogen, i.e. a single proton. Since a typical adult is approximately 60% water and 16% fat it is possible to create images which are sensitive to the protons within water and fat molecules. MRI uses three magnetic fields to create images.

The first is a strong typically 1.5 T or 3 T static magnetic field (known as B_0) that creates a weak net nuclear magnetisation within the human body. Such strong magnetic fields are achieved using superconducting magnets, although lower field strength magnets, e.g., $\lesssim 0.4$ T, are available using rare-earth permanent magnets. The net magnetisation precesses around B_0 with a characteristic frequency given by $\omega_0 = \gamma B_0$. This is known as the Larmor frequency after Joseph Larmor who in 1897 (long before NMR was discovered) proposed that charged particles should precess about a magnetic field and that the frequency of precession should be directly proportional to the field strength. In the case of NMR the constant of proportionality is γ, the gyromagnetic ratio, which is 42.47 MHz for the nucleus of ^{1}H. At 3 T, for example, the Larmor frequency is 128 MHz, i.e. in the radiofrequency (RF) part of the electromagnetic spectrum.

Since the net magnetisation is aligned along the same direction as B_0 (which shall be defined as the z-direction here) it is necessary to rotate the magnetisation so that it is aligned orthogonal to B_0. This is achieved by applying a short duration 'pulse' of a second external magnetic field (known as B_1) that is also orthogonal to B_0 and is alternating with a frequency that is equal to the Larmor frequency, i.e. it is resonant with the precessional frequency of the net magnetisation. The B_1 field is created using a transmitting RF antenna, more usually called a transmit coil. For example, a simple solenoidal coil position at right angles to B_0 would create an alternating magnetic field orientated along the length of the coil as described by Fleming's right hand thumb rule. The desired rotation of the net magnetisation about the axis of B_1 is controlled by the amplitude and duration of this transmitted RF pulse. Once the

RF pulse has been switched off the precessing transverse magnetisation induces an electromotive force (emf) in the solenoidal coil, which would now be considered a receive coil. This emf or signal is then amplified and digitised to create the MRI raw data. Immediately after the RF excitation the net magnetisation will return to thermal equilibrium via processes known as relaxation. The net transverse magnetisation will decay exponentially with a time constant called T_2, whilst the magnetisation will recover along the z-direction with a time constant known as T_1. It is the variation in T_1 and T_2 relaxation times in different tissues that is exploited in MRI to create images with differential signal intensities between tissues, e.g. the grey and white matter in the brain. In biological tissues the T_1 relaxation time is approximately an order of magnitude longer than the T_2 relaxation time. Combinations of transmitted RF pulses are used to weight the amplitude of the signal induced in the receive coil to highlight either T_1 or T_2 relaxation processes or other contrast mechanisms (figure 7).

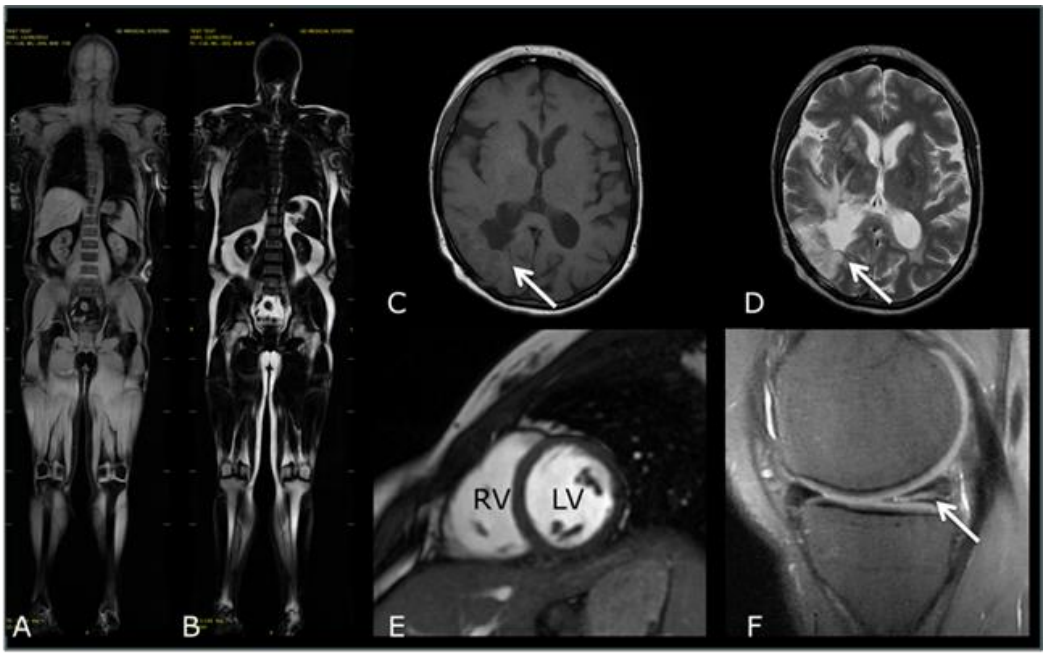

Figure 7. Some clinical MRI examples. A) is a whole-body MRI scan representing the distribution of the protons in water and B) an image showing the distribution of the protons in fat. C) is a T_1-weighted image of a patient with a brain tumour (arrow) that is difficult to identify. D) is a T_2-weighted image at the same location showing a high signal from the tumour. E) is a single frame from a cine movie of the heart as it beats. The blood in the right ventricle (RV) and the left ventricle (LV) is bright whilst the surrounding heart muscle (myocardium) is darker. F) shows a sagittal view through a knee. The femur is at the top and the tibia at the bottom with the meniscus between them. The arrow is pointing to a torn meniscus.

The third and final magnetic field used in MRI is a spatially varying magnetic field superimposed on B_0. To form an MR image it is necessary to have three linear magnetic field gradients aligned along the physical x, y and z directions. These gradient magnetic fields are created using another set of coils inside the bore of the magnet. These gradients are switched on and off to spatially encode the MR signal induced in the receiver coil. It is the switching of these gradient pulses that gives rise to the characteristic knocking noises heard during an MRI examination. There are three logical gradients used in a typical MRI acquisition referred to as slice selection, phase encoding and frequency encoding. Each logical gradient is mapped to the relevant physical axis depending upon the orientation of the acquisition plane,

i.e. axial, coronal and sagittal. Single and double oblique orientations may also be obtained by appropriate rotation of the logical gradients. The standard method of acquiring MRI images known as 'spin-warp' uses gradient pulses to encode position into the frequency and phase of the MR signal. This means that the images can be reconstructed by a straightforward Fourier transformation.

Most of the initial development work for MRI was performed in the UK with four main groups taking delivery of whole-body air-cored resistive magnets around the same time in 1977. Three were academic comprising John Mallard at the University of Aberdeen, and Peter Mansfield and Raymond Andrew leading separate groups in Nottingham. The final system was for EMI led by Hugh Clow. The first in vivo MR images started to appear in 1977. Damadian produced an image of the chest using a very different approach that did not involve magnetic field gradients, known as the FONAR (Field fOcused Nuclear mAgnetic Resonance) method [25]. Because the uniformity of Damadian's magnetic field was so poor the FONAR method utilised a small volume in the centre of the magnet where the field produced the desired Larmor frequency. The patient was then physically translated through this volume to build up the image. The academic groups initially created their images using a line scanning method, whilst the EMI group implemented a projection reconstruction method as originally used in the EMI CT scanner, producing their first successful image of the head in September 1978. The next major development was the so-called 'spin-warp' method invented at the University of Aberdeen (William Edelstein, James Hutchison et al. 1980). This technique rapidly became the basis for most MRI acquisitions and remains so to this day.

Figure 8. The original Aberdeen Mark 1 MRI scanner. Note how the patient is positioned between rather than through the magnet windings. Image taken in the Suttie Art Space in Aberdeen Royal Infirmary where the device has been on display since February 2016. AndyGaskell, CC BY-SA 4.0 <https://creativecommons.org/licenses/by-sa/4.0>, via Wikimedia Commons.

The Medical Research Council (MRC) initially funded both Nottingham groups and the Aberdeen group, whilst EMI once again approached the DHSS and the insightful Gordon Higson. By late 1978 the DHSS had agreed to contribute £350,000 on a cost sharing basis with EMI to develop a system around a 0.3 T superconducting magnet to be installed in the Royal Postgraduate Medical School (RPMS) at Hammersmith Hospital after Atkinson Morley declined to take the system ostensibly due to the number of visitors a new system would attract. The 'Neptune' system was installed in the RPMS in January 1981 with images appearing shortly thereafter [26]. In October 1979 EMI merged with Thorn Electrical Industries Ltd to form Thorn EMI. In 1980 Thorn EMI sold the CT business to the US General

Electric (GE) company and the Neptune project to Picker International Ltd. Picker began in 1909 when New York druggist James Picker first supplied Kodak X-ray plates and accessories to local hospitals. In 1958 the Picker family sold the business to CIT Financial Corporation who then sold Picker to the RCA Corporation in 1980 who in turn shortly afterwards sold it to the UK General Electric Company (GEC) (not to be confused with the US GE). GEC combined Picker with several other of its subsidiaries to form Picker International. In 1999 the company changed its name to Marconi Medical Systems as GEC attempted to rebrand itself under the Marconi name to differentiate itself from the US GE. In 2001 Royal Philips Electronics of the Netherlands acquired Marconi Medical Systems. The other commercial venture was a spin-out of the work conducted at the University of Aberdeen when John Mallard formed a small company, M&D Technology Ltd, to sell a commercial 0.08 T version of the original 0.04 T G air-cored resistive magnet [27] (figure 8). This system was unique in that the magnet was oriented so that B_0 was vertical and the patient was positioned between the two middle solenoid coils making up the magnet. Three systems were sold, one to Edinburgh Royal Infirmary, one to a private clinic in Geneva and one to St Bartholomew's Hospital (Barts) in London (the system on which the author started his MRI career in 1984). The Barts' system is now in the Science Museum in London.

In 2003 the Nobel Prize for Physiology or Medicine was jointly awarded to Lauterbur and Mansfield "*for their discoveries concerning magnetic resonance imaging*". This was much to the chagrin of Raymond Damadian who also felt that he should have been included.

MRI technology continues to rapidly evolve with substantial developments in key MR system technologies. From a hardware perspective the standard MRI system field strength is 1.5 T with an increasing adoption of 3 T MRI system in clinical practice and research, as well as the development and regulatory approval of 7 T systems for enhanced signal-to-noise ratio (SNR) and image quality. Advancements in semiconductor power devices have enabled improvements in MR gradient and RF amplifier hardware, contributing to higher performance and lower energy consumption. New image acquisition methods include fast imaging sequences and techniques to reduce image acquisition times like parallel imaging (PI), compressed sensing (CS) and simultaneous multi-slice (SMS) imaging. There are developments in image reconstruction methods incorporating artificial intelligence (AI) and deep learning (DL) algorithms, workflow automation and advancements in methods to obtain quantitative imaging-based biomarkers of disease. Like CT there are now hybrid systems such at PET/MR and MR systems integrated with linear accelerators for image-guided radiotherapy. A comprehensive review of the many developments in MRI can be found in the article by Kabasawa [28].

5. Nuclear medicine and positron emission tomography (PET)

Nuclear medicine uses small amounts of radioactive materials to diagnose and to treat various diseases. These radioactive materials are introduced into the body by injection, swallowing or inhalation. The radiopharmaceuticals are designed to target specific organs, bones or tissues where they emit γ-rays that can be detected by special types of cameras (such as gamma cameras or PET scanners). This process allows the creation of detailed images that show the structure and function of organs and tissues. The tissue specificity arises from the range of radiation-emitting radionuclides, which can be used to label specific biomarkers, biochemicals and pharmaceuticals without disturbing their biological function. In addition the radiation can be detected above the low natural radiation background. These two aspects are fundamental to realising the tracer principle for which George de Hevesy received the Nobel Prize in Chemistry in 1943 "*for his work on the use of isotopes as tracers in the study of chemical processes*". Nuclear medicine is unique because it provides medical information that is often unavailable through other imaging procedures and it can detect diseases at an earlier stage. It is used to diagnose and to manage a wide range of conditions, including cancers, heart disease, gastrointestinal, endocrine, neurological disorders and other abnormalities within the body.

5.1. Single photon emission computed tomography (SPECT)

The emitted γ-rays are detected by a gamma camera that was invented in the 1950s by Hal O. Anger, an American engineer and biophysicist. Anger developed the first gamma-camera or Anger-camera as

it was known then in 1957 [29]. The camera uses a large crystal scintillator usually made of sodium iodide (NaI) doped with thallium, which scintillates (glows) when struck by γ-rays. The size and thickness of the crystal can affect the camera's sensitivity and resolution. Attached to the crystal are multiple photomultiplier tubes (PMTs) that detect the very weak light flashes (scintillations) from the crystal and convert them into electrical signals. The arrangement and number of PMTs can influence the spatial resolution of the image. In front of the crystal a collimator made of lead or another dense material with holes drilled through it is used to ensure that only gamma rays travelling in certain directions reach the crystal. This improves image clarity and contrast. Modern gamma cameras, now more commonly referred to as a single-photon emission computed tomography (SPECT) cameras, utilise digital systems for signal processing and image reconstruction (figure 9). These systems can handle high data rates, allowing for dynamic imaging sequences and enhanced image quality. Advanced algorithms are used for image reconstruction, analysis and display. This includes methods for correcting image artifacts, enhancing contrast and quantifying radiotracer uptake. A very common radioisotope used in nuclear medicine imaging is technetium-99m (^{99m}Tc) that emits a 140 keV γ-ray. There are numerous different ligands that can be combined with ^{99m}Tc. The ligand is chosen to have an affinity for the specific organ to be targeted. For example, the exametazime chelate of ^{99m}Tc can cross the blood–brain barrier and flow through the vessels in the brain for cerebral blood flow imaging. Other ligands include sestamibi for myocardial perfusion imaging and mercapto acetyl tri-glycine (MAG3) to evaluate renal function.

Figure 9. A dual-headed single-photon emission computed tomography (SPECT) camera circa 2006. User:Drahreg01 (https://commons.wikimedia.org/wiki/File:SiemensEcamDuet.JPG), „SiemensEcamDuet“, https://creativecommons.org/licenses/by-sa/3.0/legal code .

Many tracers have very short half-lives, i.e. the time for the radioactivity to decay by a half, so a local (on-site) method of creating the radioisotope is necessary, e.g. γ-ray emitting radioisotopes are produced in generators. Generators provide a local supply of a short-lived radioactive substance from the decay of a longer-lived parent radionuclide; hence they can be transported over longer distances. For example, ^{99m}Tc with a half-life of 6 hours can be locally extracted from the radioactive decay of molybdenum-99 (^{99}Mo) that has a half-life of 66 hours.

5.2. Positron emission tomography (PET)

PET is the most specific and sensitive means for imaging molecular interactions and pathways within the human body. The specificity arises from the range of positron-emitting radionuclides, which can be used to label specific biomarkers, biochemicals and pharmaceuticals without disturbing their biological function. The most common PET tracer is ^{18}F-FDG (Fluorodeoxyglucose) that acts as a glucose analogue and is used to localise tissues with altered glucose metabolism. ^{18}F decays by emitting a

positron that annihilates with an electron, forming two 511 keV photons produced approximately 180° apart. Other useful PET radioisotopes include gallium-68 (^{68}Ga), rubidium-82 (^{82}Rb) and carbon-11 (^{11}C) for chelation with specific ligands.

Positron-emitting radionuclides are commonly produced in very expensive charged particle accelerators, e.g. linear accelerators or cyclotrons [30]. The production of ^{11}C with a half -life of 20.4 minutes will require a local cyclotron, whereas ^{18}F has a half-life of 109.7 minutes and can be shipped from a commercial supplier further afield. On-site production of tracers requires sophisticated production facilities that use automated kits provided by the cyclotron companies with the tracers synthesised in shielded containment chambers known as hot cells.

A PET scanner comprises a ring of lutetium (Lu)-based scintillation detectors and multiple PMTs or solid-state detectors that detect the photon scintillations from the crystal and convert them into electrical signals. The near simultaneous (typically within a timing window of 6 to 12 ns) detection of the two photons means that it is possible to localise their source along a straight line of coincidence (also called the line of response or LoR). In practice the LoR has a non-zero width as the emitted photons are not exactly 180° apart. Pairs of photons that do not arrive within the timing window are ignored. If the resolving time of the detectors is less than 500 ps it is possible to localise the event to a segment of a chord whose length is determined by the detector timing resolution. As the timing resolution improves the signal-to-noise ratio (SNR) of the image will improve, requiring fewer events to achieve the same image quality.

PET images are reconstructed by coincidence events being grouped into projection images called sinograms. The sinograms are sorted by the angle and for 3D images the tilt of the LoR. The sinogram images are analogous to the transmission projections acquired by a CT scanner and can be reconstructed in a similar way (figure 10). The main confounding factors are the requirements to correct for the effect of scatter of the photons and the attenuation of photons by the tissue.

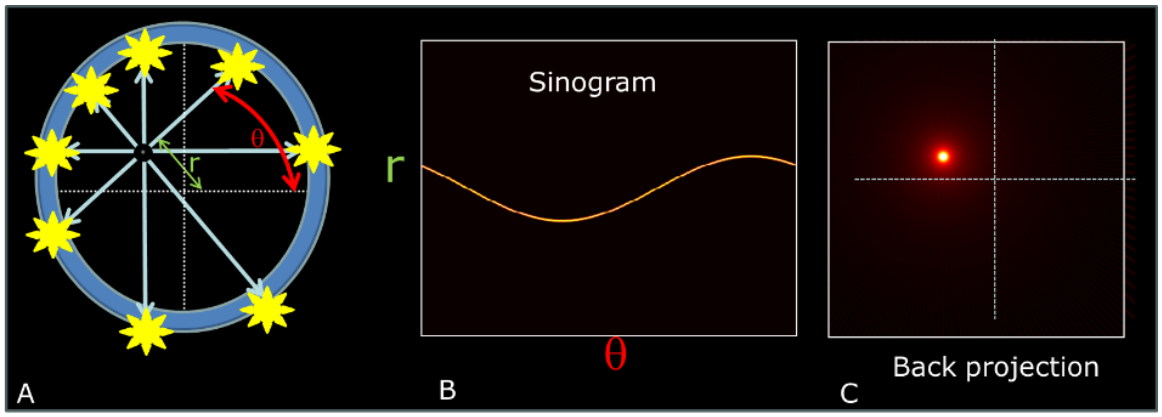

Figure 10. A) shows four coincidence detections in a PET scintillator and the lines of response from a point source of a positron-emitting radionuclide. B) shows the associate sinogram as a function of the angle θ and distance r from the centre of the PET ring. C) shows the results of back projecting the LoRs. The resultant image of the point source is blurred because a filtered back projection algorithm was not used.

Although the development of positron emitting radioisotopes detected initially by pairs of detectors can be traced back to 1951 [31], the first PET system that could make quantitative measurements of the regional tissue concentration of a PET tracer was built by Michel Ter-Pogossian, Michael Phelps, Edward Hoffman and Nizar Mullani around 1974 at Washington University [32] with Department of Energy (DoE) and National Institutes of Health (NIH) support.

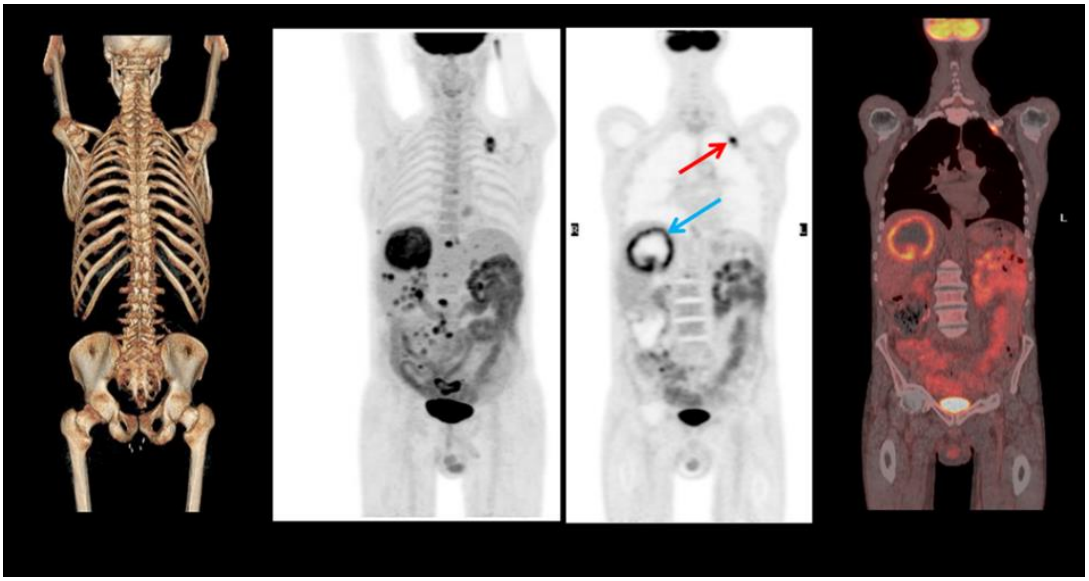

Figure 11. Images from a ^{18}F-FDG PET/CT examination. A) shows a 3D rendering of the bones from the CT acquisition. B shows a projection of all the data in the PET acquisition using an inverted greyscale. C) shows a single slice from the PET acquisition showing a large tumour in the patients' liver. There is high activity (dark ring around the tumour) around the margins of the tumour where it is rapidly growing (blue arrow). The centre of the tumour is necrotic, i.e. dead, and appears as low activity (bright centre). D) shows a fusion of the PET data (in shades of red) fused with the CT data (in grayscale) clearly showing the regions of uptake. Note a high signal in the patient's rib (red arrow).

Ter-Pogossian is recognised to have "*led the research that turned the positron emission tomography (PET) scanner from an intriguing concept to a medical tool used in hospitals and laboratories everywhere.*" [33]. Phelps, who is often credited with inventing PET, received the 1998 Enrico Fermi Presidential Award for his work. The first whole-body PET scanner appeared in 1977.

PET cameras are nowadays integrated with a CT scanner, creating a PET/CT. This has two main advantages. Firstly, the relatively low spatial resolution PET image is fused with the higher resolution CT image to show accurately where in the human body the PET tracer is localised. Secondly, the information from the CT scan can be used to determine the attenuation of the photons as they pass through the body, thereby improving the quantification of the tracer (figure 11).

Currently PET scanners record around 1% of the coincident pairs of emitted photons. Extending the length of the PET detector ring would substantially increase the system sensitivity. A commercial total-body PET system is now available with an axial field-of-view (FOV) of 200 cm compared to a typical current generation system with a FOV of 25 cm, improving sensitivity by a factor of 40 [34].

6. Ultrasound: Listening to the body

In the 1940s and 1950s ultrasound emerged as a new imaging modality. Ultrasound uses high-frequency sound waves greater than 20 kHz to create images of the inside of the body such as a fetus during pregnancy. The advantage of ultrasound is that it does not use ionising radiation, making it safer for certain applications particularly in obstetrics. The first published work on medical ultrasonics was by Karl Theodore Dussik in Austria in 1942 on transmission ultrasound investigation of the brain [35]. Much of the development of ultrasound in clinical practice was initiated by Ian Donald, Regius Professor of Midwifery at the University of Glasgow who together with his colleagues began a series of studies that would firmly establish a role for ultrasound in clinical diagnostics. Donald initially attempted to use an ultrasound device that was used in the Glasgow shipyards for testing welds in large pressure vessels

to distinguish between fibroids and cysts. Tom Brown, a research and development engineer with Kelvin & Hughes Ltd who made the ultrasound flaw detector, offered to help. Brown realised that some form of pictorial imaging was needed and believed that it might be possible to make radar-like images of internal organs. Brown conceived and designed the low-cost prototype which was to be the first direct contact ultrasound scanner and had it built onto a borrowed hospital bed table in the firm's workshops. The prototype was made available to Donald, assisted by John MacVicar, in early 1957. They quickly realised its potential and began exploring its clinical applications, publishing their first paper in June 1958 [36].

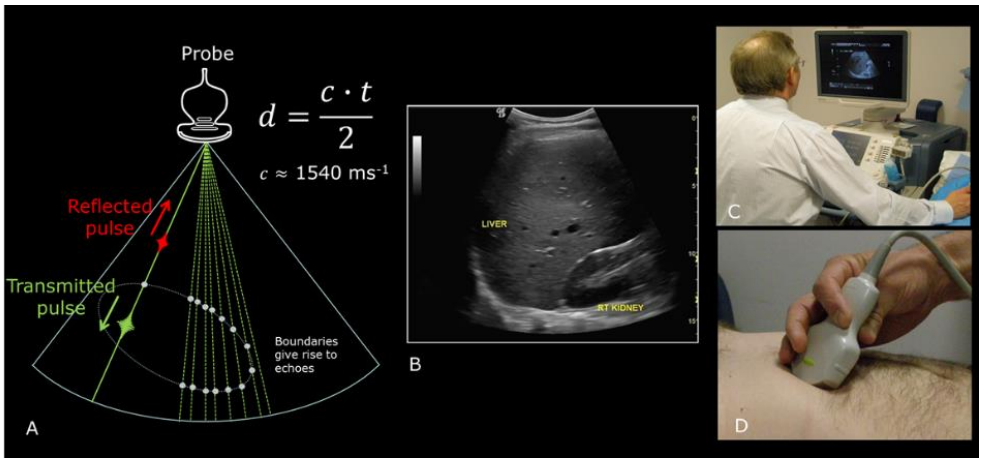

Figure 12. A) shows the basic principles behind ultrasound. A pulse of ultrasound from the transducer travels through the tissue at an approximate velocity (c) of 1540 ms-1. At a tissue interface a proportion of the ultrasound energy (the echo) is reflected to the probe whilst the remainder continues to be transmitted and will be proportionately reflected at the next tissue interface. The distance travelled by the ultrasonic pulse is given by the velocity (c) multiplied by the time (t) between the pulse and the echo divided by 2. B) shows an ultrasound image of the liver and right kidney. C) shows a radiologist using an ultrasound machine. Since ultrasound is a real-time imaging method the radiologist views the images whilst they move the probe over the patient's body as shown in D.

An ultrasound machine has a transducer probe that is used to send and to receive pulses of sound waves. When the probe is placed on the skin it emits pulses of high-frequency sound waves that propagate through the body and when they encounter different tissues (such as organs and blood vessels) some of the sound waves are reflected while others continue to travel further until they hit other boundaries and are also reflected. These reflected signals or echoes are processed to create real-time images or videos of the internal structures of the body. Image reconstruction involves algorithms that calculate the distance from the probe to the tissue boundaries by considering the speed of sound in the tissues and the time it took for the echoes to return. The amplitude of the returning echoes is highly dependent on the density and composition of tissues that the sound waves have encountered, creating contrast in the image, e.g. distinguishing between different types of tissues, fluids and other structures (figure 12).

The dynamic nature of ultrasound images allows for the observation of the structure and movement of the body's internal organs, as well as blood flowing through blood vessels. It can be used for a variety of diagnostic purposes, including examining the heart, kidneys, liver, blood vessels, pregnant uterus and other organs, guiding procedures such as biopsies and assessing fetal development during pregnancy. Ultrasound is preferred for many conditions because it does not use ionising radiation, making it safer than X-rays, particularly for pregnant women and the developing fetus. It is versatile, relatively low cost and can be performed at the bedside.

Advancements in ultrasound technology include the development of compact ultrasound probes that can connect to smartphones or tablets, effectively transforming them into portable ultrasound devices (figure 13). This innovation allows for real-time imaging to be performed almost anywhere, making diagnostic medical imaging more accessible, especially in remote areas or in situations where traditional ultrasound machines are not available. These mobile-connected ultrasound devices are being increasingly used in diverse medical fields for quick assessments, emergency diagnostics and in settings with limited access to conventional imaging facilities.

Figure 13. A pocket-sized ultrasound device. Images are displayed on a smartphone via a device-generated wireless connection. Under a Creative Commons (CC) license permission to publish this picture was obtained from HEALCERION, Seoul, Korea (S2 File). https://doi.org/10.1371/journal.pone.0185031.g001 .

7. Digital imaging and advances

The late 20th and early 21st centuries have seen significant advances in digital imaging techniques, enhancing the quality and accessibility of medical images. Digital technology has also facilitated the development of telemedicine, allowing for remote diagnostics and consultation. Artificial Intelligence (AI) has started and will continue to play a significant role in modern medical imaging, revolutionising how images are acquired, reconstructed and interpreted, leading to improvements in how diseases are diagnosed and how patient care is delivered [37]. AI algorithms can analyse medical images more quickly and accurately than traditional methods. Through training on huge volumes of annotated data, they can detect patterns and anomalies that might be missed by the human eye and have shown high accuracy in identifying various conditions, including cancers, neurological disorders and cardiovascular diseases. They can help in reducing diagnostic errors, potentially resulting in earlier diagnosis and improving patient outcomes. AI can streamline medical imaging workflows, reducing the time radiologists spend on image analysis. Automated report generation and prioritisation of cases based on urgency are examples where AI aids in managing the clinical workload more effectively. AI systems are increasingly integrated with hospital electronic health records (EHRs) to provide a more comprehensive view of a patient's medical history, improving diagnostic accuracy and facilitating personalised medicine.

However, despite its potential the integration of AI into medical imaging faces challenges, including regulatory hurdles and the need for large annotated datasets for training as well as concerns about data privacy and security. Furthermore, ensuring AI models are transparent, explainable and unbiased remains a priority to gain trust from healthcare professionals and patients alike.

8. Conclusion

From the discovery of X-rays to the advent of AI in imaging the field of medical imaging has undergone remarkable transformations. Each advancement has opened new possibilities for diagnosis and treatment, significantly impacting patient care. As technology continues to evolve the future of medical

imaging promises even greater innovations, including the development of more sophisticated AI algorithms that can provide real-time diagnostics, the integration of imaging data with genomic information for personalised medicine, and the creation of less invasive imaging techniques that offer higher resolution and clearer insights into the human body. The convergence of imaging technology with other fields such as nanotechnology and biotechnology may lead to breakthroughs in early detection and treatment of diseases at a molecular level. Moreover, the increasing accessibility of advanced imaging technologies in remote areas through mobile and cloud-based solutions will be likely to democratise healthcare, making high-quality diagnostics available to a broader population. Ultimately the ongoing integration of AI and other innovative technologies in medical imaging holds the promise of transforming healthcare delivery, making it more predictive, personalised and accurate.

References

[1] Röntgen W K 1895 Über eine neue Art von Strahlen : vorläufige Mitteilung *Sitzungsber. Phys. Med. Gesell.*
[2] Rowland S and Hammond Smith H 1896 Report on the application of the new photography to medicine and surgery *The British Medical Journal* **1** 874
[3] Oestreich A E 1995 Professor William F. Magie and the American discovery of the fluoroscope, 1896 *AJR Am. J. Roentgenol.* **165** 1060
[4] Anonymous 1896 The Edison X ray experiments, apparatus and fluoroscope *Sci. Am.* **74** 219
[5] Oldendorf W 1961 Isolated flying spot detection of radiodensity discontinuities—displaying the internal structural patterns of a complex object *IRE Trans. Biomed. Electron.* **8** 68
[6] Oldendorf W 1963 US Patent No. 3,106,640
[7] Oldendorf W 1991 The continued quest for an image of brain *J. Neuroimaging* **1** 46
[8] Oldendorf W H 1980 *The quest for an image of brain* (New York: Raven Press).
[9] Cormack A M 1963 Representation of a function by its line integrals, with some radiological applications. I *J. App. Phys.* **34** 2722
[10] Cormack A M 1964 Representation of a function by its line integrals, with some radiological applications. II *J. App. Phys.* **35** 2908
[11] Beckmann E C 2006 CT scanning the early days *Br. J. Radiol.* **79** 5
[12] Schulz R A *et al.* 2021 How CT happened: the early development of medical computed tomography *Journal of Medical Imaging,* **8**
[13] Hounsfield G N 1968 UK Patent No. 1,283,915
[14] Hounsfield G N 1971 US Patent No. 3,778,614
[15] Ambrose J and Hounsfield G N 1973 Computed transverse tomography *Br. J. Radiol.* **46** 148
[16] Strong A B and Hurst R A 1994 EMI patents on computed tomography: history of legal actions *Br. J. Radiol.* **67** 315
[17] Isherwood I 2004 Sir Godfrey Hounsfield – Nobel Laureate *Eur. Radiol.* **14** 2152
[18] Booij R *et al.* 2020 Technological developments of X-ray computed tomography over half a century: User's influence on protocol optimization *Eur. J. Radiol.* **131** 109261
[19] Lell M M and Kachelriess M 2020 Recent and upcoming technological developments in computed tomography: High speed, low dose, deep learning, multienergy *Invest. Radiol.* **55** 8
[20] Hsieh J and Flohr T 2021 Computed tomography recent history and future perspectives *J Med Imaging (Bellingham)* **8** 052109
[21] Willemink M J *et al.* 2018 Photon-counting CT: Technical principles and clinical prospects *Radiology* **289** 293
[22] Bloch F *et al.* 1946 Nuclear induction *Physical Review* **69** 127
[23] Purcell E M *et al.* 1946 Resonance absorption by nuclear magnetic moments in a solid *Physical Review* **69** 37
[24] Lauterbur P C 1973 Image formation by induced local interactions: examples employing nuclear magnetic resonance *Nature* **242** 190
[25] Damadian R *et al.* 1977 NMR in cancer: XVI. FONAR image of the live human body *Physiol.*

Chem. & Phys. **9** 97
[26] Higson G R 1987 Seeing things more clearly *Br. J. Radiol.* **60** 1049
[27] Mallard J R 2006 Magnetic resonance imaging-the Aberdeen perspective on developments in the early years *Phys. Med. Biol.* **51** R45
[28] Kabasawa H 2022 MR imaging in the 21st Century: Technical innovation over the first two decades *Magn. Reson. Med. Sci.* **21** 71
[29] Anger H O 1958 Scintillation Camera *Rev. Sci. Instrum.* **29** 27
[30] Saha G B *et al.* 1992 Cyclotrons and positron emission tomography radiopharmaceuticals for clinical imaging *Semin. Nucl. Med.* **22** 150
[31] Wrenn F R *et al.* 1951 The use of positron-emitting radioisotopes for the localization of brain tumors *Science* **113** 525
[32] Ter-Pogossian M M *et al.* 1975 A positron-emission transaxial tomograph for nuclear imaging (PETT) *Radiology* **114** 89
[33] Wackers F J T 2018 Michael M. Ter-Pogossian (1925-1996) *J. Nucl. Cardiol.* **25** 1090
[34] Jones T and Townsend D 2017 History and future technical innovation in positron emission tomography *J Med Imaging (Bellingham)* **4** 011013
[35] Dussik K T 1942 On the possibility of using ultrasound waves as a diagnostic aid. *Z Neurol Psychiatr* **174** 153
[36] Donald I *et al.* 1958 Investigation of abdominal masses by pulsed ultrasound *Lancet* **1** 1188
[37] Najjar R 2023 Redefining radiology: A review of artificial intelligence integration in medical imaging *Diagnostics (Basel)* **13**